Singlet oxygen stimulates mitochondrial bioenergetics in brain cells

Sergei G Sokolovski[2], Edik U. Rafailov[2], Andrey Y. Abramov[1], Plamena R. Angelova[1,*]

[1]*Department of Clinical and Movement Neurosciences, UCL Institute of Neurology, Queen Square, London WC1N 3BG, UK*

[2]*Aston Institute of Photonics Technologies, Aston University, UK*

**correspondence to: Dr Plamena R. Angelova, p.stroh@ucl.ac.uk*

Keywords

1267nm, singlet oxygen, energy metabolism, mitochondrial respiration, brain

Abstract

Oxygen, in form of reactive oxygen species (ROS), has been shown to participate in oxidative stress, one of the major triggers for pathology, but also is a main contributor to physiological processes. Recently, it was found that 1267nm irradiation can produce singlet oxygen without photosensitizers. We used this phenomenon to study the effect of laser-generated singlet oxygen on one of the major oxygen-dependent processes, mitochondrial energy metabolism. We have found that laser-induced generation of $^1O_2$ in neurons and astrocytes led to the increase of mitochondrial membrane potential, activation of NADH- and FADH-dependent respiration, and importantly, increased the rate of maximal respiration in isolated mitochondria. The activation of mitochondrial respiration stimulated production of ATP in these cells. Thus, we found that the singlet oxygen generated by 1267nm laser pulse works as an activator of mitochondrial respiration and ATP production in the brain.

Introduction

Energy generation in the form of ATP in the cells of our body meets the specific energy demands of different types of tissues. Brain is relatively small (~1-2% of body weight) organ but consumes ten times more oxygen and glucose than any other organ in order to cover its huge energy needs. Oxygen is predominantly consumed in the electron transport chain of mitochondria in a process which is coupled with the production of ATP, i.e. oxidative phosphorylation. Such a high level of oxygen and changes in metabolic conditions can generate free radicals, e.g. superoxide anion or any other form of ROS (1). Evolutionary mitochondria, and cells in general, have developed an effective antioxidant system, which successfully protects neurons and other cells against oxidative damage. It is well known that oxidative stress plays a pivotal role in the etiopathology of many disease (2-4). However, cells are also utilizing ROS in number of physiological processes, predominantly for signalling (1, 2, 5) and in cell stimulation (6). While a signalling role for superoxide or hydrogen peroxide have been described in detail, far less is known about the possible role of some other ROS, including hydrogen anion radical or singlet oxygen, in health and disease. The role of singlet oxygen in physiology and the development of pathology is much less established due to technical limitations, not allowing a thorough study, compared to the rest of the reactive oxygen species.

Singlet oxygen is the common name of an electronically excited state of triplet oxygen (lowest excited state of the dioxygen molecule) which is less stable than molecular oxygen in the electronic ground state. Despite its high reactivity, the lifetime of $^1O_2$ in water solutions (7) is higher than most of the other ROS, with exception of hydrogen peroxide (8). Considering this, singlet oxygen can be involved in a number of physiological processes as a signalling and stimulatory molecule or in the same reactions as triplet oxygen, but with higher reactivity and, possible efficiency. Singlet oxygen is shown to be formed in cellular enzymatic reactions in a range of peroxidase enzymes including myeloperoxidase, lactoperoxidase, chloroperoxidase, during lipoxygenase-catalysed reactions (9); (10, 11).

Potentially $^1O_2$ can be decomposed from lipid hydroperoxides (12, 13). As well, singlet oxygen can be formed in cells “environmentally”, when UVA irradiation is absorbed by endogenous sensitizers (14). However, main knowledge of the cellular effects of singlet oxygen came from photodynamic therapy (PDT) experiment (15), where externally administered and light-activated photosensitizers excite $^3O_2$ to $^1O_2$ or release $^1O_2$ by thermal decomposition of 3,3'-(1,4-naphthylidene) dipropionate endoperoxide (NDPO2) (16). Photosensitizers are also capable of producing a number of other reactive oxygen species and demonstrated their own intrinsic and photo-toxicity which could be beneficial predominantly for purpose of tumour tissue damage but not very helpful in the unravelling of the specific effects of singlet oxygen on cell metabolism and immunity (17, 18). Wavelength of 1262–1268 nm coincides with one of the highest absorption peaks of the oxygen molecule transforming it into singlet oxygen without photosensitizers (19); (20); (21). This property is used for the development of lasers in this spectrum, allowing for the generation of highly specific tool to study the role of singlet oxygen in physiology, pathology and as a highly promising instrument for therapy (18, 22, 23).The ability of the infrared laser pulse of 1267 nm to produce singlet oxygen in organic solution and in cancer cell line has clearly been demonstrated (17).

Here, we studied of the effects of singlet oxygen generated by the 1267 nm laser irradiation on mitochondrial metabolism and bioenergetics of brain cells.

Results

In agreement with previous publications, we have found that 1267 nm induced the production of singlet oxygen in primary neurons and astrocytes (Figure 1).

Thus, loading control cells with Si-DMA results in the oxidation of this indicator, followed by fluorescence in the mitochondrial area (Figure 1a).1267 nm laser irradiation in the dose-dependent manner increased the rate of singlet oxygen production in neurons and

astrocytes (Figure 1 c). Interestingly, the highest level of Si-DMA fluorescence intensity was also observed in mitochondria and vesicle-like structures (Figure 1b, c).

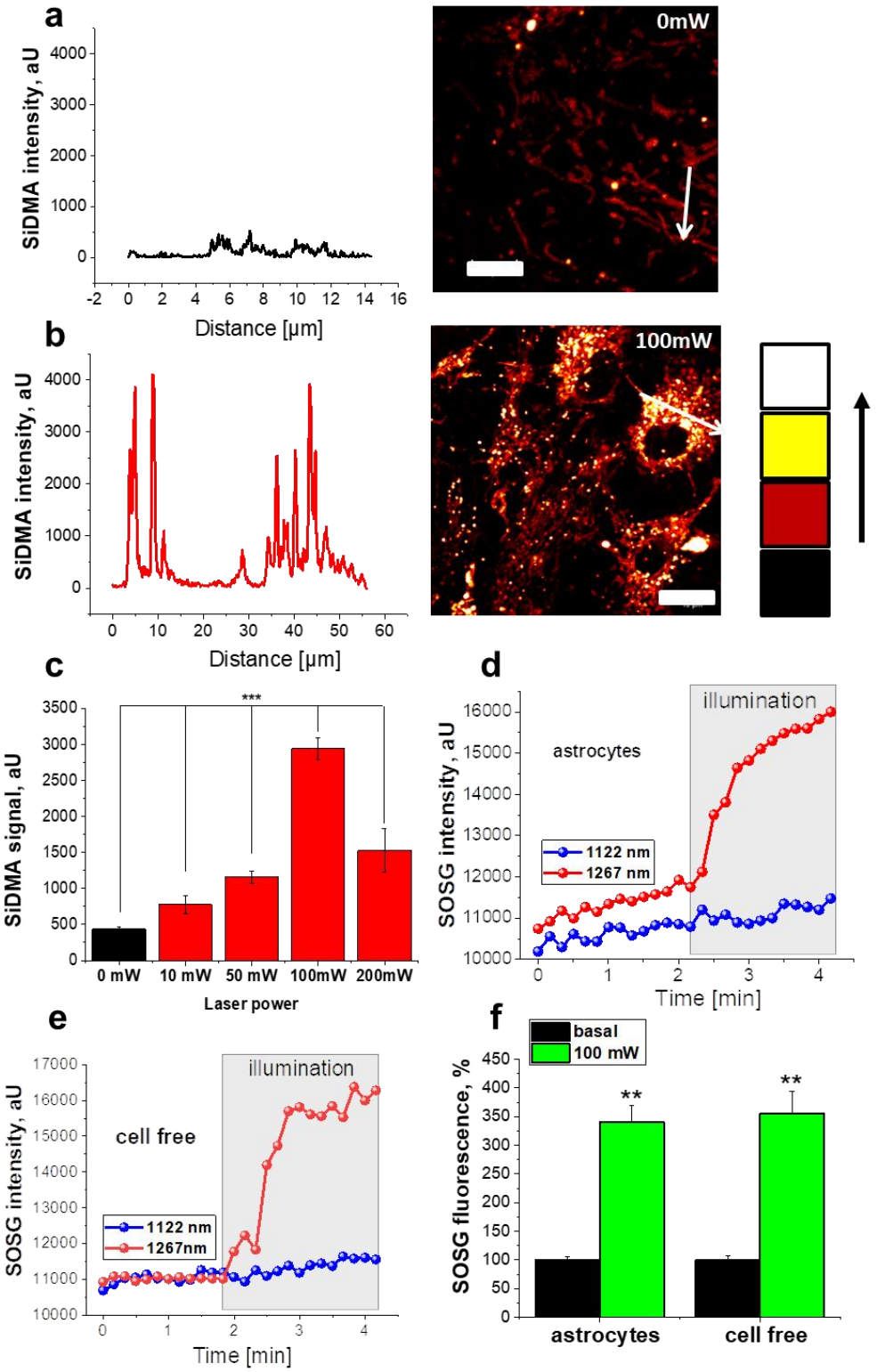

Figure 1: Singlet oxygen production by 1267nm laser illumination in neurons and astrocytes. *a) Intensity profile of Si-DMA singlet oxygen indicator in an astrocyte at 0 J/cm². Intensity the profile represents the area under the arrow on the image (right). Scale bar: 10 µm. Pseudocoloured fluorescence images of Si-DMA distribution in brain cells. b-Intensity profile of Si-DMA (singlet oxygen indicator) in an astrocyte after illumination with 1267 nm*

*for 2 min at 71 mW (65.0 J/cm^2). Intensity profile represents the area under the arrow on the pseudocoloured fluorescence image (right). Fluorescence increase especially along mitochondria and vesicle-like structures is evident. Scale bar: 10 µm. c-Dose- dependent effect of 1267nm laser irradiation on the level of Si-DMA fluorescence. N ≥ 4 experiments. d-e. Representative traces of the effect of 129.2 J/cm^2 irradiation dose induced by 1122nm and 1267 nm lasers on the Singlet Oxygen Sensor Green (SOSG) fluorescence in cell-free HBSS solution (d) and in cortical astrocytes (e). f- Summary of the effect of laser irradiation (129.2 J/cm^2) on the SOSG fluorescence as a percentage of basal level. Error bars indicate SEM; *p < 0.01; **p < 0.001; ***p < 0.0001.*

Importantly, illumination of co-culture of neurons and astrocytes with a 1122 nm laser (control) with a relatively close water absorption coefficient, did not change Si-DMA fluorescence intensity, even at high laser power outputs (>141 mW, 129.2 J/cm^2). The data on singlet oxygen production with Si-DMA were confirmed using another indicator – Singlet Oxygen Sensor Green (Figure 1 d-f). Thus, illumination of the HBSS containing this fluorescent probe without cells by 1267 nm laser (129.2 J/cm^2) induced more than 3.5-fold increase in the rate of fluorescence while 1122 nm laser did not induce any changes in the same conditions (N=5 experiments; Figure 1 d, f). Importantly, none of the mitochondrial inhibitors (5 µM rotenone or 0.2 mg/ml oligomycin) or uncoupler (1 µM FCCP) had any effects on the Singlet Oxygen Sensor Green fluorescence in cell-free solution.

This indicates that in our experimental conditions, the observed effects have been associated with singlet oxygen produced by the 1267 nm laser only.

1267 nm laser pulse increases mitochondrial membrane potential

Mitochondrial bioenergetics is a temperature-dependent process, therefore all our experiments were executed under strict temperature control (t=25.0±0.05°C), using a Laser Diode Driver with TEC (thermoelectric cooler element). Mitochondrial membrane potential (∆ψm) is an indicator of mitochondrial “health” and functionality. We used TMRM (tetramethylrhodamine, 25 nM) as a fluorescent probe to report ∆ψm in primary cortical neurons and astrocytes. Irradiation of cells with 1267 nm laser-induced dose-dependent increase of mitochondrial membrane potential, in both neurons and astrocytes (Figure 2 a, b). High–power laser illumination of Rhodamine-based fluorescent indicators is also one of

the common methods for generation of superoxide anion and for the triggering of mitochondrial permeability transition pore opening -mPTP, (4). Similarly, we have found that at high dose ranges (>205 mW; 187.8 J/cm^2) of 1267 nm irradiation induces a transient drop in $\Delta\psi m$ of astrocytes and neurons that can be seen even in single mitochondria (see Figure 2 c). This suggests that singlet oxygen production by 1267 nm irradiation at comparably high doses, is toxic for mitochondria, and evokes mitochondrial PTP opening. Thus, the irradiation of primary neurons and astrocytes with 1267 nm laser induced a profound, dose-dependent mitochondrial hyperpolarisation followed by a transient depolarisation at higher doses (>205mW, 187.8 J/cm^2).

Singlet oxygen production by 1267 nm laser activates consumption of mitochondrial NADH and FADH

NADH is a substrate and a donor of electrons for complex I of the mitochondrial Electron Transport Chain (ETC). Measurement of NADH autofluorescence in live single cells gives information about the activity of ETC in general and about complex I, in particular. Exposure of co-cultured neurons and astrocytes to 37.18 mW (32.47 J/cm^2) of 1267nm laser irradiation did not change the level of NADH autofluorescence (Figure 2 d). However, increase of the power intensity to 71 mW (2 min, 62.0 J/cm^2) or 141 mW (2min, 123.1 J/cm^2) induced 20-30 % decrease in mitochondrial NADH pool (Figure 2 d). Decrease in NADH redox levels can be induced by activation of mitochondrial respiration and acceleration of NADH consumption by complex I (24) or by activation of NAD consumption by enzyme PARP after stimulation with ROS (25); (26). Decrease in mitochondrial NADH (Figure 2 d) is more likely due to activation of ETC because 71 mW (2 min, 62.0 J/cm^2) or 141 mW (2 min, 123.1 J/cm^2) irradiation with 1267 nm also induced increase in FAD autofluorescence (Figure 2 e) that corresponds to activation of the mitochondrial complex II.

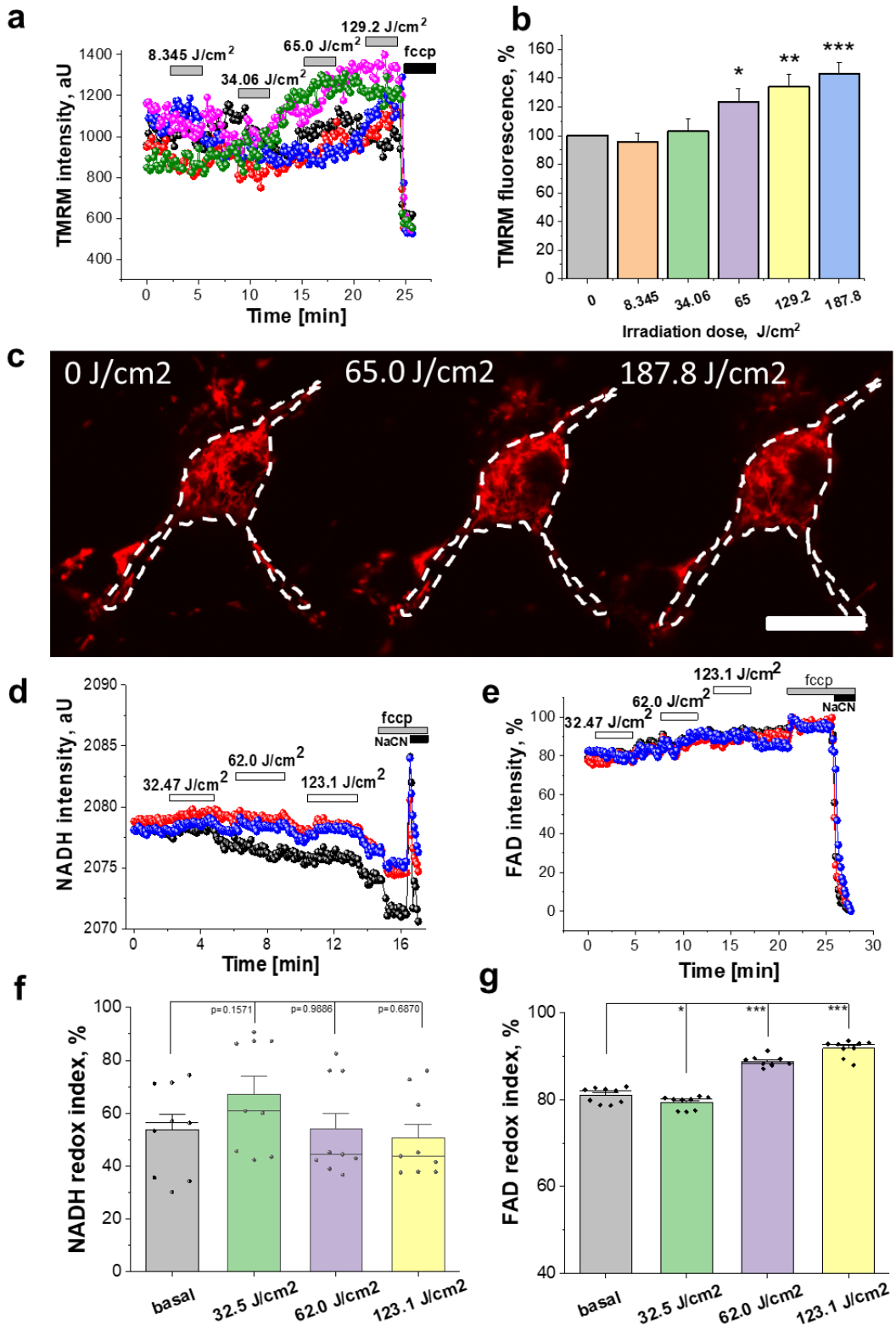

Figure 2: 1267 nm irradiation increased mitochondrial membrane potential and activated NADH- and FADH-dependent respiration. *a) TMRM measurements reveal increase in mitochondrial membrane potential in brain cells upon 1267 nm illumination. b) Bar charts representing the mitochondrial membrane potential dependence on the irradiation dose. N ≥ 4 experiments. Error bars indicate SEM; *p < 0.05; **p < 0.001; ***p < 0.0001. c) Representative fluorescence images of TMRM-loaded neuron challenged with 1267nm pulses at different intensities. Scale bar: 10 µm. d) Representative NADH autofluorescence measurements reveal increased respiration in brain cells upon 1267 nm*

*illumination. e) FAD autofluorescence is also increased upon application of different doses of 1267 nm irradiation. Summary of the NADH (e) and FAD (f) redox indices, calculated as a percentage of basal autofluorescence from experiments shown in representative detail in d) and e). Error bars indicate SEM; *p < 0.05; **p < 0.001; ***p < 0.0001; N ≥ 4 experiments.*

Application of 1 µM FCCP in the end of experiments maximised mitochondrial respiration and minimised the level of NADH (but increased FAD^{++} due to a decrease in FADH), while 1 mM NaCN inhibited mitochondrial respiration, blocked NADH and FADH consumption and gave a maximal (and minimal for FAD) value for mitochondrial NADH (Figure 2 d, e). It should be noted that irradiation of primary cortical co-culture of neurons and astrocytes with a control laser of 1122 nm did not cause any changes in NADH or FAD autofluorescence. Thus, production of singlet oxygen by 1267 nm laser pulse leads to activation of the ETC complex I and complex II of mitochondria in live neurons and astrocytes.

Singlet oxygen production by 1267 nm laser irradiation increases ATP production in primary neurons and astrocytes

The effect of 1267 nm laser–induced $^1O_2$ generation on mitochondrial respiration in single cells results in acceleration of the ATP production. Thus, laser irradiation of 71 mW intensity power (65.0 J/cm^2) moderately increases intracellular ATP levels, which is presumably absorbed by the cell antioxidant systems after switching the laser off (Figure 3 a). Increasing the laser power to 141 mW (129.2 J/cm^2), and further (after a 3-4 minutes pause), to 205 mW (187.8 J/cm2) stimulated ATP synthesis in neurons (Figure 3 a) and astrocytes (Figure 3 b) bringing it to a plateau. Inhibition of ATP production in the cells with inhibitor of oxidative phosphorylation oligomycin (2mg/ml) and inhibitor of glycolysis iodo-acetic acid (IAA, 20 µM) induced a significant drop of ATP in these cells confirming the effect of singlet oxygen on the cell ATP production (Figure 3 a, b).

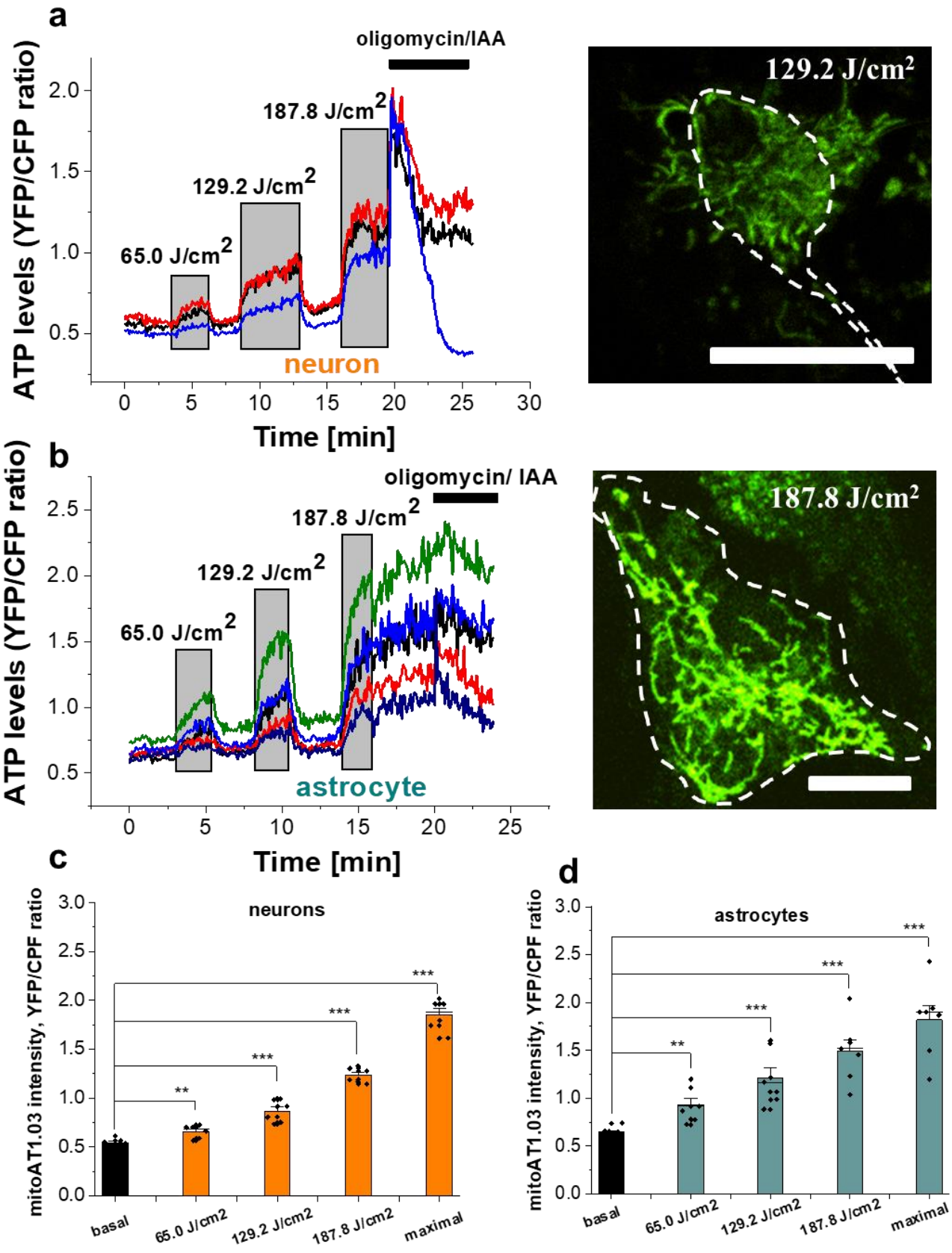

Figure 3: 1267nm irradiation stimulates ATP production in mixed neuroglial culture. ***a)*** *Neurons: ATP levels upon illumination with a 1267nm pulse at different intensities (grey bars) in neuronal cultures using a FRET-based mitochondrial ATP probe. Note the reduction of the signal after application of inhibitors of ATP synthesis, 2mg/ml oligomycin and 20 µM iodoacetic acid (IAA). Representative image of a neuron transfected with the mitochondrial*

ATP probe and subjected to 1267 nm illumination at 141 mW (129.2 J/cm^2). Scale bar: 50 µm. b) Astrocytes: Representative trace of kinetic changes in mitochondrial ATP of astrocyte while being illuminated with a 1267nm pulse at different intensities in neuroglial co-cultures. Note the reduction of the signal after application of inhibitors of oxidative phosphorylation, 2mg/ml oligomycin and 20 µM iodoacetic acid (IAA). Representative image of an astrocyte transfected with the mitochondrial ATP after 1267 nm illumination at 141 mW (187.2 J/cm^2). Scale bar: 20 µm. Quantification bar charts of experiments of different 1267 nm laser doses on the production of ATP in c) neurons and d) astrocytes.

Direct effect of 1267nm laser-generated singlet oxygen on the respiration of isolated mitochondria

Exposure of isolated rat brain mitochondria to 1267 nm laser induced a dose-dependent activation of the oxygen consumption in mitochondria in glutamate/malate containing medium (Figure 4 a, b). Singlet oxygen produced by the 1267 nm laser activates ADP-dependent (V3) and ADP independent (V4) respiration of mitochondria, without significant changes in the respiratory control ratio, suggesting that activation of respiration is not induced by mitochondrial uncoupling (Figure 4 c). Intriguingly, the exposure of mitochondria to 1267 nm irradiation increased ADP/O ratio (Figure 4 a) pointing towards an enhanced efficiency of oxidative phosphorylation of these mitochondria. Activation of maximal mitochondrial oxygen consumption by application of 0.5 µM FCCP showed that in mitochondria irradiated with 1267 nm laser the rate of mitochondrial respiration is significantly higher than in control (Figure 4 d, e).

One should also note that Clark electrode allows for registering the production of singlet oxygen as a process opposed to the oxygen consumption in the chamber, as shown in an experiment in mitochondria-free solution, following 1267 nm illumination (f). It strongly suggests that singlet oxygen does not alter proteins of the electron transport chain (ETC) but activates it and increases the efficiency of ATP production, supposedly through an F0-F1-ATPase activity modulation.

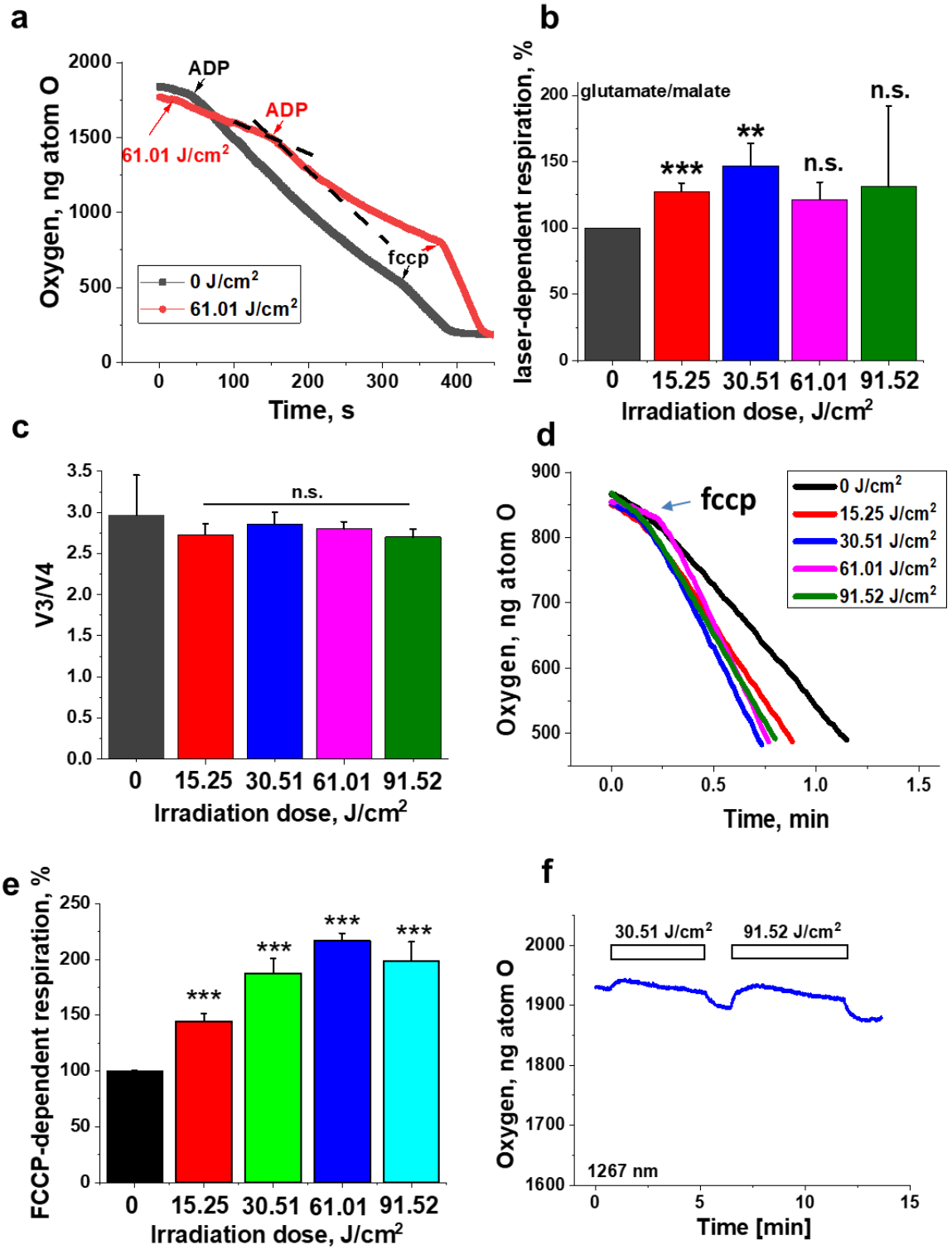

Figure 4: 1267nm laser application increases the efficiency of oxidative phosphorylation. *a),b) dose-dependent activation of the oxygen consumption in mitochondria in glutamate/malate containing medium upon 1267nm illumination. N ≥ 4 experiments. Error bars indicate SEM; n.s. non-significant; **p < 0.001; ***p < 0.0001. c) No significant (n.s.) changes in respiratory control ratio (RCR, V3/V4) after application of a 1267 nm laser pulse at different power intensities. d), e) maximal mitochondrial oxygen consumption (after application of 0.5 µM fccp) is further activated in mitochondria with 1267 nm pulses of variable power intensities. N ≥ 4 experiments. Error bars indicate SEM; n.s. non-significant; **p < 0.001; ***p < 0.0001. f) Effect of 2 different doses of 1267nm*

illumination on the oxygen level in a chamber of Clark electrode in the absence of mitochondria.

Discussion

The positive effects of singlet oxygen on the mitochondrial bioenergetics, which we observe here, could be detected because of recent developments in optical technology, which allow us to deliver singlet oxygen (without the introduction of photosensitisers or significant production of other ROS) to the cells. Toxic effects of singlet oxygen on mitochondria (including opening of the mitochondrial permeability transition pore (16); (27) or positive effects (28) were studied using different approaches and, unfortunately, not always could be directly compared.

Such specific and positive effects of singlet oxygen on mitochondrial energy metabolism are probably highly specific for this particular form of oxygen, because general oxidative stress activates respiration via mitochondrial uncoupling, induced by lipid peroxidation; or by inhibition of respiration due to direct action of the laser-generated ROS on mitochondrial complexes or by limitation of mitochondrial substrates by DNA-repairing enzymes (25, 26, 29).

Although redox activation of Nrf2 can lead to stimulation of mitochondrial bioenergetics (24);(30) almost immediate effect of 1267 nm laser irradiation is less likely due to effect on the Nrf2 pathway.

There are two possible explanations of the activation of mitochondrial respiration by singlet oxygen: a) activation of the complexes I and II (donors of electron for ETC) by flavin semiquinone ($FADH^{\bullet}$) and superoxide ($O_2^{\bullet -}$) or singlet oxygen spin-correlated radical pair (28) or/and by b) modifying effect of singlet oxygen on the cytochrome C oxidase activity (31); (32).

Also, singlet oxygen can inhibit mitochondrial superoxide dismutase and catalase (33, 34) that potentially should increase the level of superoxide and H_2O_2 in the matrix of

mitochondria (35). In combination with NO it could produce peroxynitrite that has been shown to be an inhibitor of mitochondrial respiration (36). However, in our experiments production of singlet oxygen stimulated mitochondrial respiration therefore an effect of superoxide anion or peroxynitrite formation under these conditions could be ruled out.

Production of singlet oxygen and superoxide anion by NADH:coenzyme Q reductase and aldehyde oxidase activates the formation of metal-protein complexes (37) that can also be relevant for proteins of ETC and may be an additional trigger for activation of respiration by laser-induced singlet oxygen.

Activation of mitochondrial respiration by laser irradiation of 100-300 mW (30.51—91.52 J/cm^2) is more likely not associated with typical mitochondrial uncoupling because of the increase in ATP levels and the relatively stable respiratory control ratio (RCR). Considering this, we could exclude effect of singlet oxygen in these dose ranges on uncoupling proteins or lipid peroxidation, which can modify membrane conductance. Interestingly, similar effects on the ATP level and mitochondria has been observed with helium-neon laser irradiation, at 632 nm, one of the absorption peaks for molecular oxygen (38) or with 441 nm (39); which is far from singlet oxygen absorption wavelengths. In fact, there is a large body of evidence that lasers from the near infrared spectrum range and beyond, are effective in stimulating mitochondrial respiration, hyperpolarizing mitochondrial membranes and, as an end-effect, increasing the production of ATP (40-43). The main target of these molecular effects appears to be mitochondrial cytochrome C oxidase, or complex IV of the mitochondrial ETC. Although various studies, reporting the optimisation of mitochondrial respiration and the stimulation of the ATP production by low-level laser illumination in various types of cells and tissues have been published, there is still a gap in the knowledge and an essential need to identify the exact mechanism by which laser irradiation leads to these effects. Here, we made a good step further into elucidating the 1267nm laser mechanism of action by bringing the singlet oxygen into the complex equation of cell energy metabolism.

To our understanding mild and constant ROS generation is an essential part of cell signalling and feedback mechanisms in the brain (1, 44-46). This signalling and feedback loop properties of the brain system is especially important in abnormal conditions or chronic diseases in the brain, like neurodegeneration or ischaemia for example, where severe lack of energy production in the form of ATP is a hallmark of pathology (47).

Methods

Laser specification

For the experiments in this study we have used a CW fibre coupled single-mode laser diode (Innolume, Germany) emitting at 1267nm. The power intensities varied from 1 to 300 mW by controlling applied current on a device and monitoring by a feedback photodiode. Compact Laser Diode and Temperature Controller (CLD with TEC; ThorLabs) was used for the supply of drive current and the maintenance of the fiber-coupled laser diode temperature with 0.005 °C stability. A linewidth of emission wavelength was around 0.5 nm. Laser illumination was applied using the following sequence of: 2 min – irradiation, 2 min – pause. We have calculated the doses, obtained by the cellular and mitochondrial preparations, according to: dose=P*t/(S/cos45) [J/cm^2], using the following parameters for different experimental settings:

Table 1. Dose calculation parameters

	CCD camera experiments	Confocal microscope experiments		Oxygen sensor experiments
Power Distance Beam diameter	Doses, J/cm^2 L=12cm D=3.5173mm	Doses, J/cm^2 L=3.5cm D=3.4342mm	Power Distance Beam diameter	Doses, J/cm^2 L=4cm D=1.25mm
9.11 mW	7.96	8.345	10mW	3.05
37.18 mW	32.47	34.06	50mW	15.25
71 mW	62.0	65.0	100mW	30.51
141 mW	123.1	129.2	200mW	61.01
205 mW	179.0	187.8	300mW	91.52

Illumination time for all experiments was 120s, except otherwise stated.

Cell culture preparation

Co-cultures of cortical neurons and astrocytes were prepared as described previously (48) with modifications, from Sprague-Dawley rat pups 0–2 days post-partum (UCL breeding colony). Experimental procedures were performed in compliance with the United Kingdom Animals (Scientific Procedures) Act of 1986. Brain cortices were removed into ice-cold HBSS and the tissue was minced and trypsinised, triturated and plated on poly-D-lysine-coated coverslips. The cultures were maintained at 37 °C (5% CO_2) and cells were used at 12–15 days in vitro.

Live cell imaging

Mitochondrial singlet oxygen production was assessed using Si-DMA (Dojindo, Japan) without application of photosensitiser. 1 μM Si-DMA was loaded into cells at 37°C for 30 min and imaged, excited with 633 nm laser line of Zeiss 710 VIS CLSM. Mitochondrial membrane potential was measured using potential sensitive indicator tetramethylrhodamine (TMRM; (49). Cells were loaded with 20 nM TMRM for 40 min at room temperature, excited at 565 nm and imaged with a 580 nm emission filter as previously described. Illumination intensity was kept to a minimum (at 0.1–0.2% of laser output) to avoid phototoxicity and the pinhole set to give an optical slice of ~2 μm. TMRM is used in the redistribution mode to assess $\Delta\Psi m$, and therefore a reduction in TMRM fluorescence represents mitochondrial depolarisation.

NADH autofluorescence was monitored using an epifluorescence inverted microscope equipped with a × 40 fluorite objective. Excitation light (350 nm) was provided by a Xenon arc lamp, the beam passing through a monochromator (Cairn Research, Kent, UK). Emitted fluorescence light was reflected through a 455-nm long-pass filter to a cooled CCD camera (Retiga, QImaging, Canada). Imaging data were collected and analysed using software from Andor (Belfast, UK). FAD++ autofluorescence was monitored using a Zeiss 710 VIS CLSM and a × 40 objective. We used 454nm laser for excitation with emission at 505–550 nm.

Experimental protocols and data analysis were performed as described in (50).To determine the ATP levels, primary co-cultures were transfected with a mitochondrial ATP probe (COX1.03) generated by Imamura and colleagues, using Effectene (Qiagen) according to the manufacturer's instructions. The FRET was quantified by the 527:475 nm ratio with an excitation of 405 nm and a filter from 515 to 580 nm (51).

Isolation of mitochondria

Mitochondria were isolated from the brain of Sprague–Dawley rats (150-200 g, UCL breeding colony) as described in (52) with some modifications. Experimental procedures were performed in compliance with the United Kingdom Animals (Scientific Procedures) Act of 1986. Animal studies were approved by the UCL ethical committee and performed under a U.K. Home Office project license. Briefly, the animals were euthanized by cervical dislocation, brain was taken out, homogenized and re-suspended in isolation buffer (300 mM sucrose, 2 mM EDTA, and 5 mM Tris-HCl, pH 7.4). Mitochondria were isolated by differential centrifugation at +1° C temperature. Nuclei and intact cells were centrifuged for 10 minutes at 800×g. Resulting supernatant was centrifuged for 20 minutes at 20000×g. The pellet was re-suspended in 500 µl of isolation buffer without EDTA and put on ice.

Oxygen consumption

Oxygen consumption was measured in a Clark-type oxygen electrode (Hansatech) according to (53), thermostatically maintained at 25°C containing the following (in mM): 135 KCl, 10 NaCl, 20 HEPES, 0.5 KH2PO4, 1 MgCl2, and 5 EGTA, pH 7.1. Glutamate (5 mM), malate (5 mM), and sodium succinate (5 mM) were added to allow basal respiration (V2). Data were obtained using an Oxygraph Plus system with Chart recording software. Protein levels were established using a Pierce BCA protein assay kit (recordings were adjusted accordingly). The respiratory control parameter was calculated as the ratio of metabolic States V_3 to V_4 (V3/V4). V_2 or V_{sub} - mitochondrial respiration rate in the presence of

substrates without ADP; V_3 - mitochondrial respiration rate activated by the addition of ADP; V_4 - mitochondrial respiration rate in the presence of substrates after all added ADP was converted to ATP; V_{FCCP} – maximal respiration rate in presence of uncoupler FCCP. ADP/O was calculated as the ratio of 50 µMoles of ADP (converted by mitochondria to ATP) to the amount of oxygen (µg) used during oxidative phosphorylation process (V3).

Data and statistical analysis

Statistical analysis and data analysis were performed using Origin 9 (Microcal Software Inc., Northampton, MA) and Prism 7 (GraphPad Software, San Diego, CA) software. Kolmogorov-Smirnov test was used to assess data normality. Statistical analysis was performed using unpaired two-tailed Student's t-test. Results are expressed as means ± standard error of the mean (S.E.M.). Differences were considered to be significantly different at $p < 0.05$.

Acknowledgements

The authors acknowledge the support of the Engineering and Physical Sciences Research Council (EPSRC) (Grant No. EP/R024898/1).

Author's contributions

E.U.R. and **A.Y.A.** initiated and supervised this work. **S.S.; E.U.R.**: Provision of laser instrumentation, dose calulation, Writing – Reviewing.
A.Y.A. Conceptualization, Methodology, Writing - original draft preparation;
P.R.A.: Investigation, Data curation, Formal analysis,Visualisation; Writing – Reviewing & Editing.

Declaration of Interests

The authors declare no competing interests.

References

1. Angelova PR, Abramov AY. Functional role of mitochondrial reactive oxygen species in physiology. Free Radic Biol Med. 2016;100:81-5.
2. Angelova PR, Abramov AY. Role of mitochondrial ROS in the brain: from physiology to neurodegeneration. FEBS Lett. 2018;592(5):692-702.
3. Deas E, Cremades N, Angelova PR, Ludtmann MH, Yao Z, Chen S, et al. Alpha-Synuclein Oligomers Interact with Metal Ions to Induce Oxidative Stress and Neuronal Death in Parkinson's Disease. Antioxid Redox Signal. 2016;24(7):376-91.
4. Ludtmann MHR, Angelova PR, Horrocks MH, Choi ML, Rodrigues M, Baev AY, et al. alpha-synuclein oligomers interact with ATP synthase and open the permeability transition pore in Parkinson's disease. Nat Commun. 2018;9(1):2293.
5. Domijan AM, Kovac S, Abramov AY. Lipid peroxidation is essential for phospholipase C activity and the inositol-trisphosphate-related Ca(2)(+) signal. J Cell Sci. 2014;127(Pt 1):21-6.
6. Nishinaka Y, Arai T, Adachi S, Takaori-Kondo A, Yamashita K. Singlet oxygen is essential for neutrophil extracellular trap formation. Biochemical and Biophysical Research Communications. 2011;413(1):75-9.
7. Zakharov SD, Ivanov AV, Wolf EB, Danilov VP, Murina TM, Nguen KT, et al. Structural rearrangements in the aqueous phase of cell suspensions and protein solutions induced by a light-oxygen effect. Quantum Electron. 2003;33(2):149-62.
8. Lindig B. A. MAJR, and A. Paul Schaap. Determination of the Lifetime of Singlet Oxygen in D20 Using 9,10-Anthracenedipropionic Acid, a Water-Soluble Probe. J Am Chem Soc. 1980;102:5590-3.
9. Davies MJ. Reactive species formed on proteins exposed to singlet oxygen. Photochem Photobiol Sci. 2004;3(1):17-25.
10. Kanofsky JR. Singlet oxygen production by lactoperoxidase. J Biol Chem. 1983;258(10):5991-3.
11. Kanofsky JR, Wright J, Miles-Richardson GE, Tauber AI. Biochemical requirements for singlet oxygen production by purified human myeloperoxidase. J Clin Invest. 1984;74(4):1489-95.
12. Girotti AW. Lipid hydroperoxide generation, turnover, and effector action in biological systems. J Lipid Res. 1998;39(8):1529-42.
13. Miyamoto S, Martinez GR, Martins AP, Medeiros MH, Di Mascio P. Direct evidence of singlet molecular oxygen [O2(1Deltag)] production in the reaction of linoleic acid hydroperoxide with peroxynitrite. J Am Chem Soc. 2003;125(15):4510-7.
14. Davies SS, Amarnath V, Roberts LJ, 2nd. Isoketals: highly reactive gamma-ketoaldehydes formed from the H2-isoprostane pathway. Chem Phys Lipids. 2004;128(1-2):85-99.
15. Diamond I, Mcdonagh A, Wilson C, Granelli S, Nielsen S, Jaenicke R. Photodynamic therapy of malignant tumours. The Lancet. 1972;300(7788):1175-7.
16. Cosso RG, Turim J, Nantes IL, Almeida AM, Di Mascio P, Verces AE. Mitochondrial permeability transition induced by chemically generated singlet oxygen. J Bioenerg Biomembr. 2002;34(3):157-63.
17. Sokolovski SG, Zolotovskaya SA, Goltsov A, Pourreyron C, South AP, Rafailov EU. Infrared laser pulse triggers increased singlet oxygen production in tumour cells. Sci Rep. 2013;3:3484.
18. Khokhlova A, Zolotovskii I, Stoliarov D, Vorsina S, Liamina D, Pogodina E, et al. The Photobiomodulation of Vital Parameters of the Cancer Cell Culture by Low Dose of Near-IR Laser Irradiation. IEEE Journal of Selected Topics in Quantum Electronics. 2019;25(1):1-10.

19. Zakharov SDaAVI. Light-oxygen effect in cells and its potential applications in tumour therapy Quantum Electronics. 1999;20(12):192–214
20. Zakharov SD, V. A. Ivanov, E. B. Wolf, V. P. Danilov, T. M. Murina, K. T. Nguen,, E. G. Novikov NAP, S. N. Perov, S. A. Skopinov, Yu. P. Timofeev. Structural rearrangements in the aqueous phase of cell suspensions and protein solutions induced by a light-oxygen effect. Quantum Electronics. 2003;33(2):149–62.
21. Gudkov SV, Bruskov VI, Astashev ME, Chernikov AV, Yaguzhinsky LS, Zakharov SD. Oxygen-dependent auto-oscillations of water luminescence triggered by the 1264 nm radiation. J Phys Chem B. 2011;115(23):7693-8.
22. Khokhlova A, Zolotovskii I, Sokolovski S, Saenko Y, Rafailov E, Stoliarov D, et al. The light-oxygen effect in biological cells enhanced by highly localized surface plasmon-polaritons. Scientific Reports. 2019;9(1):18435.
23. Semyachkina-Glushkovskaya O, Kurths J, Borisova E, Sokolovski S, Mantareva V, Angelov I, et al. Photodynamic opening of blood-brain barrier. Biomed Opt Express. 2017;8(11):5040-8.
24. Holmstrom KM, Baird L, Zhang Y, Hargreaves I, Chalasani A, Land JM, et al. Nrf2 impacts cellular bioenergetics by controlling substrate availability for mitochondrial respiration. Biol Open. 2013;2(8):761-70.
25. Abramov AY, Duchen MR. Mechanisms underlying the loss of mitochondrial membrane potential in glutamate excitotoxicity. Biochim Biophys Acta. 2008;1777(7-8):953-64.
26. Delgado-Camprubi M, Esteras N, Soutar MP, Plun-Favreau H, Abramov AY. Deficiency of Parkinson's disease-related gene Fbxo7 is associated with impaired mitochondrial metabolism by PARP activation. Cell Death Differ. 2017;24(12):2210.
27. Salet C, Moreno G, Ricchelli F, Bernardi P. Singlet oxygen produced by photodynamic action causes inactivation of the mitochondrial permeability transition pore. J Biol Chem. 1997;272(35):21938-43.
28. Usselman RJ, Chavarriaga C, Castello PR, Procopio M, Ritz T, Dratz EA, et al. The Quantum Biology of Reactive Oxygen Species Partitioning Impacts Cellular Bioenergetics. Sci Rep. 2016;6:38543.
29. Abramov AY, Duchen MR. Impaired mitochondrial bioenergetics determines glutamate-induced delayed calcium deregulation in neurons. Biochim Biophys Acta. 2010;1800(3):297-304.
30. Ludtmann MH, Angelova PR, Zhang Y, Abramov AY, Dinkova-Kostova AT. Nrf2 affects the efficiency of mitochondrial fatty acid oxidation. Biochem J. 2014;457(3):415-24.
31. Kim J, Rodriguez ME, Guo M, Kenney ME, Oleinick NL, Anderson VE. Oxidative modification of cytochrome c by singlet oxygen. Free Radic Biol Med. 2008;44(9):1700-11.
32. Estevam ML, Nascimento OR, Baptista MS, Di Mascio P, Prado FM, Faljoni-Alario A, et al. Changes in the spin state and reactivity of cytochrome C induced by photochemically generated singlet oxygen and free radicals. J Biol Chem. 2004;279(38):39214-22.
33. Escobar JA, Rubio MA, Lissi EA. Sod and catalase inactivation by singlet oxygen and peroxyl radicals. Free Radic Biol Med. 1996;20(3):285-90.
34. Kim SY, Kwon OJ, Park JW. Inactivation of catalase and superoxide dismutase by singlet oxygen derived from photoactivated dye. Biochimie. 2001;83(5):437-44.
35. Radi R, Turrens JF, Chang LY, Bush KM, Crapo JD, Freeman BA. Detection of catalase in rat heart mitochondria. J Biol Chem. 1991;266(32):22028-34.
36. Lizasoain I, Moro MA, Knowles RG, Darley-Usmar V, Moncada S. Nitric oxide and peroxynitrite exert distinct effects on mitochondrial respiration which are differentially blocked by glutathione or glucose. Biochem J. 1996;314 (Pt 3):877-80.
37. Kerver ED, Vogels IM, Bosch KS, Vreeling-Sindelarova H, Van den Munckhof RJ, Frederiks WM. In situ detection of spontaneous superoxide anion and singlet oxygen

production by mitochondria in rat liver and small intestine. Histochem J. 1997;29(3):229-37.
38. Iaffaldano N, Paventi G, Pizzuto R, Di Iorio M, Bailey JL, Manchisi A, et al. Helium-neon laser irradiation of cryopreserved ram sperm enhances cytochrome c oxidase activity and ATP levels improving semen quality. Theriogenology. 2016;86(3):778-84.
39. Osipov AN, Stepanov GO, Vladimirov YA, Kozlov AV, Kagan VE. Regulation of cytochrome C peroxidase activity by nitric oxide and laser irradiation. Biochemistry (Mosc). 2006;71(10):1128-32.
40. Castano AP, Demidova TN, Hamblin MR. Mechanisms in photodynamic therapy: part two-cellular signaling, cell metabolism and modes of cell death. Photodiagnosis Photodyn Ther. 2005;2(1):1-23.
41. Desmet KD, Paz DA, Corry JJ, Eells JT, Wong-Riley MT, Henry MM, et al. Clinical and experimental applications of NIR-LED photobiomodulation. Photomed Laser Surg. 2006;24(2):121-8.
42. Rojas JC, Gonzalez-Lima F. Low-level light therapy of the eye and brain. Eye Brain. 2011;3:49-67.
43. Chung H, Dai T, Sharma SK, Huang YY, Carroll JD, Hamblin MR. The nuts and bolts of low-level laser (light) therapy. Ann Biomed Eng. 2012;40(2):516-33.
44. Novikova IN, Manole A, Zherebtsov EA, Stavtsev DD, Vukolova MN, Dunaev AV, et al. Adrenaline induces calcium signal in astrocytes and vasoconstriction via activation of monoamine oxidase. Free Radic Biol Med. 2020;159:15-22.
45. Angelova PR, Muller WS. Arachidonic acid potently inhibits both postsynaptic-type Kv4.2 and presynaptic-type Kv1.4 IA potassium channels. Eur J Neurosci. 2009;29(10):1943-50.
46. Angelova P, Muller W. Oxidative modulation of the transient potassium current IA by intracellular arachidonic acid in rat CA1 pyramidal neurons. Eur J Neurosci. 2006;23(9):2375-84.
47. Abramov AY, P.R. A. Mitochondrial dysfunction and energy deprivation in the mechanism of neurodegeneration Turkish Biochemical Journal. 2019;44(6).
48. Angelova PR, Vinogradova D, Neganova ME, Serkova TP, Sokolov VV, Bachurin SO, et al. Pharmacological Sequestration of Mitochondrial Calcium Uptake Protects Neurons Against Glutamate Excitotoxicity. Mol Neurobiol. 2018.
49. Angelova PR, Barilani M, Lovejoy C, Dossena M, Vigano M, Seresini A, et al. Mitochondrial dysfunction in Parkinsonian mesenchymal stem cells impairs differentiation. Redox Biol. 2018;14:474-84.
50. Arber C, Angelova PR, Wiethoff S, Tsuchiya Y, Mazzacuva F, Preza E, et al. iPSC-derived neuronal models of PANK2-associated neurodegeneration reveal mitochondrial dysfunction contributing to early disease. PLoS One. 2017;12(9):e0184104.
51. Imamura H, Nhat KP, Togawa H, Saito K, Iino R, Kato-Yamada Y, et al. Visualization of ATP levels inside single living cells with fluorescence resonance energy transfer-based genetically encoded indicators. Proc Natl Acad Sci U S A. 2009;106(37):15651-6.
52. Ludtmann MH, Angelova PR, Ninkina NN, Gandhi S, Buchman VL, Abramov AY. Monomeric Alpha-Synuclein Exerts a Physiological Role on Brain ATP Synthase. J Neurosci. 2016;36(41):10510-21.
53. Kinghorn KJ, Castillo-Quan JI, Bartolome F, Angelova PR, Li L, Pope S, et al. Loss of PLA2G6 leads to elevated mitochondrial lipid peroxidation and mitochondrial dysfunction. Brain. 2015;138(Pt 7):1801-16.